Lifetimes of the First Excited States of Li^7 and Be^7†

P. PAUL, J. B. THOMAS,* AND S. S. HANNA
Department of Physics, Stanford University, Stanford, California
(Received 24 January 1966; revised manuscript received 21 March 1966)

The lifetimes of the first excited states of Li^7 and Be^7 have been remeasured with the Doppler-shift attenuation method and a lithium-drifted germanium detector. The value of the mean life obtained for Li^{7*}, $(1.06\pm0.14)\times10^{-13}$ sec, is in better agreement with earlier measurements from resonance fluorescence than with previous determinations by the Doppler-shift method. The value obtained for Be^{7*}, $(1.92\pm0.25)\times10^{-3}$ sec, agrees with but is appreciably lower and more precise than an earlier Doppler-shift measurement. The value of 1.82 ± 0.20 obtained for the ratio of the lifetimes, and the lifetimes themselves, are in excellent agreement with the range of values expected for intermediate coupling with L-S coupling predominating ($a/K<3.6$). They agree as well with specific theoretical predictions based on studies of p-shell nuclei.

I. INTRODUCTION

A COMPARISON of radiative lifetimes of analog levels in mirror nuclei can provide a sensitive test of calculations of nuclear structure. The almost pure $M1$ transitions from the first excited states of the $A=7$ nuclei (Fig. 1) are an important and well-studied case. In fact, the first application of the Doppler-shift attenuation method[1] was to the first excited state of Li^7 at 478 keV. This measurement has been repeated[2] and a measurement has been made on the analog state in Be^7 at 432 keV.[2] In addition, the lifetime of the state in Li^7 has been determined by resonance fluorescence.[3–6]

As can be seen in Table VI, values obtained previously for Li^7 with the Doppler-shift technique are in disagreement with the measurements from resonance fluorescence. This discrepancy, which occurs also in measurements on other nuclei, has usually been attributed to imperfect knowledge of the energy loss of recoiling ions in matter. Moreover, it has not been possible to obtain a direct comparison of the lifetimes in Li^7 and Be^7 in a single experiment because of the difficulty of resolving the gamma rays with energies of 478 and 432 keV with NaI detectors. Thus, a simultaneous comparison of the lifetimes has not been achieved.

The greatly improved resolution available with lithium-drifted germanium detectors now makes such a comparison feasible. In addition, the increase in precision in the Doppler-shift method resulting from improved resolution and stability, together with newer energy loss data for Li^7 ions,[7] should provide a better comparison of this method with the resonance fluorescence method. Finally, recent specific theoretical predictions[8,9] for these states make a remeasurement of the lifetimes desirable.

II. EXPERIMENTAL METHOD

In the simplest application of the Doppler-shift attenuation method,[10,11] the recoil velocities are limited to the range in which the stopping power ($-dE/dx$) is proportional to velocity, so that a characteristic slowing down time α can be defined by the relation

$$-dE/dx=-Mdv/dt=(M/\alpha)v. \quad (1)$$

The energy of a gamma ray emitted at time t after the collision is then

$$E(t,\theta_r)=E_0\{1+[v(\theta_r)/c][\cos\theta_d e^{-t/\alpha}\}. \quad (2)$$

The angles are defined in Fig. 2. The distribution of excited recoils in time is $e^{-t/\tau}$, where τ is the mean life. If the correlation function for emission of a recoil followed by a gamma ray is denoted by $W(\theta_r,\theta,\Phi)$, then the centroid of the energy distribution of gamma rays reaching the detector is

$$E_c(\theta)=\frac{\int\int E(t,\theta_r)W(\theta_r,\theta,\Phi)e^{-t/\tau}d\Omega_r dt}{\int\int W(\theta_r,\theta,\Phi)e^{-t/\tau}d\Omega_r dt}$$

$$=E_0\left(1+\frac{\alpha}{\alpha+\tau}\frac{\langle v_z\rangle_\theta}{c}\cos\theta\right), \quad (3)$$

where

$$\langle v_z\rangle_\theta=\int v(\theta_r)\cos\theta_r W(\theta_r,\theta,\Phi)d\Omega_r\Big/\int W(\theta_r,\theta,\Phi)d\Omega_r. \quad (4)$$

† Supported in part by the U. S. Army Research Office (Durham) and the National Science Foundation.
* National Science Foundation Predoctoral Fellow.
[1] L. G. Elliott and R. E. Bell, Phys. Rev. **76**, 168 (1949).
[2] D. St. P. Bunbury, S. Devons, G. Manning, and T. H. Towle, Proc. Phys. Soc. (London) **A69**, 165 (1956); S. Devons, Natl. Acad. Sci.—Natl. Res. Council Publ. **974**, 86 (1962).
[3] O. Beckman and R. Sandstrom, Nucl. Phys. **5**, 595 (1958).
[4] C. P. Swann, V. K. Rasmussen, and F. R. Metzger, Phys. Rev. **114**, 862 (1959).
[5] W. L. Mouton, J. P. F. Sellschop, and R. J. Keddy, Phys. Rev. **128**, 2745 (1962).
[6] E. C. Booth, B. Chasan, and K. A. Wright, Nucl. Phys. **57**, 403 (1964).
[7] Y. A. Teplova, V. S. Nikolaev, I. S. Dmitriev, and L. N. Fateeva, Zh. Eksperim. i Teor. Fiz. **42**, 44 (1962) [English transl.: Soviet Phys.—JETP **15**, 31 (1962)].
[8] S. Cohen and D. Kurath, Nucl. Phys. **73**, 1 (1965).
[9] F. C. Barker (private communication).
[10] A. E. Litherland, M. J. L. Yates, B. M. Hinds, and D. Eccleshall, Nucl. Phys. **44**, 220 (1963).
[11] E. K. Warburton, D. E. Alburger, and D. H. Wilkinson, Phys. Rev. **129**, 2180 (1963).

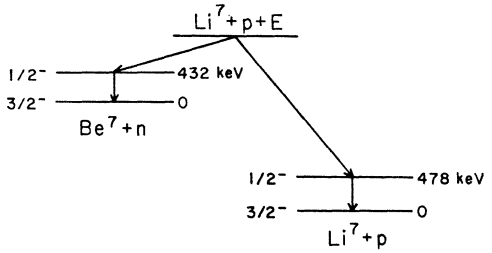

FIG. 1. Mirror transitions in Li^7 and Be^7 and the reactions used to study them.

If E_c is measured at two angles θ_1 and θ_2,

$$\Delta E_c = E_c(\theta_1) - E_c(\theta_2) = E_0[\alpha/(\alpha+\tau)](1/c) \times[\langle v_z\rangle_{\theta_1}\cos\theta_1 - \langle v_z\rangle_{\theta_2}\cos\theta_2]. \quad (5)$$

If $W(\theta_\gamma,\theta,\Phi)$ is known, $\langle v_z\rangle_\theta$ can be evaluated from Eq. (4), and then $\alpha/(\alpha+\tau)$ can be obtained from Eq. (5). If the gamma rays are emitted isotropically, as in the present case, the correlation function depends only on θ_γ and the average of the projected velocity is independent of θ.

Since the correlation function is usually not known with sufficient precision even for isotropic gamma-ray emission, an alternative procedure is to measure ΔE_c for two different stopping media, I and II. Then

$$F = \Delta E_c^{\rm I}/\Delta E_c^{\rm II} = [\alpha^{\rm I}/(\alpha^{\rm I}+\tau)][(\alpha^{\rm II}+\tau)/\alpha^{\rm II}]. \quad (6)$$

If the second medium is vacuum, $\alpha^{\rm II}=\infty$, and

$$F = \Delta E_c/\Delta E_c^{\rm vac} = \alpha/(\alpha+\tau). \quad (7)$$

The measurement is most precise if a stopping medium is used for which $\alpha\approx\tau$, and if $\langle v_z\rangle$ (see below, however) and $(\cos\theta_2-\cos\theta_1)$ are maximized, although the result is independent of these latter quantities.

Since the resolving power of a Ge(Li) detector is sufficient to reveal the Doppler broadening of the observed lines, the measurements can be analyzed in a different manner. For an observation at $\cos\theta=1$, for example, the line observed for recoils traveling in vacuum will be shifted to higher energy and broadened owing to the spread in recoil velocities (angle and magnitude). This curve can be considered as the prompt ($t=0$) resolution function of a time-delay measurement. The stopping material serves to convert time to gamma-ray energy, so that the number of decays producing gamma rays of energy E_γ is given by the expression

$$dn = AE_\gamma^{(\alpha/\tau-1)}dE_\gamma. \quad (8)$$

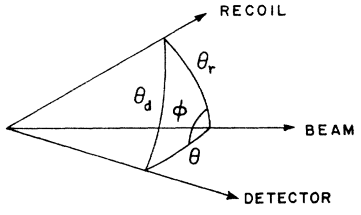

FIG. 2. Definition of angles used to describe the directions of a recoil and the detector relative to each other and to the beam in the laboratory system.

Thus, the line obtained for recoils stopping in the medium evolves from folding the prompt curve (suitably modified for decreasing velocity spread) into the function of Eq. (8). This results in a modified line shifted to lower energy, analogous to the delayed curve in a time-delay measurement. The shift in the centroid can be obtained from Eq. (3). The lifetime may also be extracted by fitting the observed line with a curve generated from Eq. (8). This procedure, illustrated later in Fig. 7, was used to obtain a sensitive and instructive check on the lifetimes and the corrections used in obtaining the lifetimes from the centroids.

The experimental technique was based on the following considerations.

1. *Reactions*

In order to make the comparison between stopping in a medium and free recoil in vacuum, it is necessary to select reactions which produce recoil distributions restricted to forward cones. The endothermic reactions $Li^7(p,p')Li^{7*}$ and $Li^7(p,n_1)Be^{7*}$ (Fig. 1) satisfy this requirement and also can produce sufficiently high recoil velocities. The reactions $H^2(Li^6,p)Li^{7*}$ and $H^2(Li^6,n)Be^{7*}$ also fulfill the requirement and would, in fact, produce somewhat larger Doppler shifts, since the recoils would have smaller relative spreads in velocity and would be restricted to narrower forward cones. However, the first pair of reactions was selected because of the availability of solid targets with a high specific Li^7 content, as compared to targets with a high specific H^2 content, and because the energy loss in a target backing (the stopping medium) is small for protons as compared to Li^6 ions. The latter consideration arises in the technique used to determine the Doppler shift for free recoil.

2. *Comparison of Doppler Shifts*

In order to make a direct comparison of the Doppler shift for recoils stopping in a medium with that for free recoil, the target backing should be just thick enough to stop the recoils but, at the same time, very thin for the incident particles of the reaction. The comparison can then be made by orienting the target in the usual way, so that the ions recoil into the backing, and then reversing the target to allow the incident beam to pass through the backing and onto the thin target, so that the ions recoil into vacuum. If the backing is very thin, the straggling and scattering of the beam will be negligible and the energy of the incident beam can be increased to compensate very accurately for the small loss of beam energy in traversing the backing.

3. *Stopping Medium*

For Li^7 and Be^7 ions, α is approximately 20×10^{-13} sec for a light stopping medium such as lithium, decreases to approximately 3×10^{-13} sec for nickel, and then re-

mains substantially constant for heavier media.[7,12,13] Thus, for the anticipated lifetimes in the range $(1\text{–}3)\times10^{-13}$ sec, a medium in the vicinity of nickel or above should be chosen. Nickel was selected since the stopping power for lithium ions in nickel has been measured and it is a convenient target backing which facilitates the measurements of the full Doppler shift for ions traveling in vacuum, as described above.

4. *Initial Recoil Velocity*

The stopping power for ions in a given medium levels off at a maximum value and finally declines with increasing velocity (see Fig. 3). Thus, when it is desirable to have maximum stopping power, as in the present case, the ideal velocity is not the largest possible. Moreover, if the method outlined above is to be used, the ideal velocity is that for which the stopping power attains its maximum value within the linear region. Since a spread of velocities is encountered in practice, it is desirable to select the range so as to maximize the stopping powers while staying in the linear region. The recoil velocities used in the experiment were in the ranges shown in Fig. 3.

5. *Target Thickness*

The equations given above are valid only for a target of zero thickness. If the time required for a recoil to traverse the target is very short compared to the mean life of the state, the effect of target thickness is negligible. Because of the low density of atoms in lithium metal or compounds, it is not possible to use targets thin enough to make the target correction negligible and at the same time maintain adequate yield and target uniformity. For a given initial velocity and path length in the target, the target correction modifies Eq. (7) as follows:

$$F_m=[\alpha/(\alpha+\tau)](1+(\tau/\alpha)f), \tag{9a}$$

where F_m is the measured shift ratio and $f=1-e^{-t_d/\tau}$ is the fraction of recoils which decay in the target. The time spent in the target is $t_d=d/v$, where d is the path length in the target and v the initial velocity. The only assumption made in obtaining Eq. (9a) is that the slowing down is negligible in the target, as is the case for lithium targets. In applying Eq. (9a) to the actual measurements, it is necessary to average f over the initial velocity distribution and over the target thickness:

$$F_m=[\alpha/(\alpha+\tau)](1+(\tau/\alpha)\langle f\rangle), \tag{9b}$$

$$F_m=[\alpha/(\alpha+\tau)](1+d/2\langle v_z\rangle\alpha), \quad (t_d\ll\tau), \tag{9c}$$

where d is now the total target thickness. In principle, an optimum target thickness is obtained by balancing the errors introduced by the target correction against the errors associated with low yield. Since the former errors are difficult to assess, measurements were made for a series of target thicknesses in order to test empirically the self-consistency of the target correction. The target correction in Eq. (9b) was computed numerically as a function of target thickness, and is shown in Fig. 4. In these calculations it is necessary to know beforehand the lifetimes of the states. These were estimated with the aid of the first-order approximation of Eq. (9c), followed by an iteration if necessary. The target thickness d was computed for a lithium metal target. In the actual calculations the very small slowing down in the target was taken into account. In obtaining the target correction it is sufficiently precise to assume isotropic angular distributions for the reaction products.

6. *Scattering of Recoils*

The method outlined above is valid if the recoils do not change direction in coming to rest in the medium. This condition is quite well fulfilled for recoil velocities above 10^8 cm/sec.[10] However, below this velocity the large-angle atomic scattering becomes progressively more serious. Thus, even though the average initial velocity is well above 10^8 cm/sec, the recoil scattering

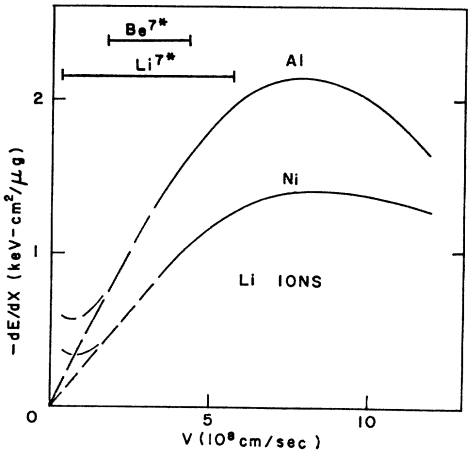

FIG. 3. Stopping powers for lithium ions in aluminum and nickel, reproduced from Ref. 7 (solid part of curves). The ranges of the recoil velocities used in most of the runs are indicated.

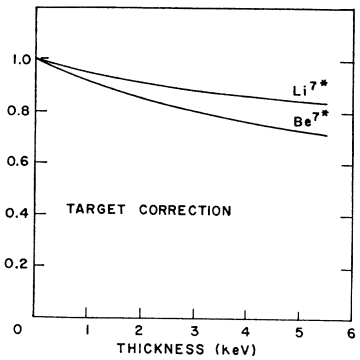

FIG. 4. Corrections for target thickness to be applied to the measured values of the shift ratio F_m. The target thickness is for 1.88-MeV protons, as measured at the $Li^7(p,n)Be^7$ threshold.

[12] D. I. Porat and K. Ramavataram, Proc. Roy. Soc. (London) A252, 394 (1959); Proc. Phys. Soc. (London) 77, 97 (1961); 78, 1135 (1961).
[13] L. C. Northcliffe, Ann. Rev. Nucl. Sci. 13, 67 (1963).

can produce a serious error if the lifetime is long enough so that many of the gamma rays are emitted from recoils whose velocities have fallen below this value. Estimates based on the conditions outlined above indicate that the effect of recoil scattering is probably negligible, but that it might possibly be important in the case of Be^{7*} because of its longer lifetime. Because of this uncertainty two runs were made in which the effect of scattering was substantially reduced. In one, the initial recoil velocities were increased, so that for Be^{7*} the recoil velocities were maximized along the linear part of the stopping power curve (see Fig. 2). In the second run, the nickel backing was replaced by carbon which has a much smaller stopping power, so that the effect of scattering should be greatly decreased since many fewer recoils decay at low velocity. (This is supported by values of the nuclear correction term listed in Table III.) As will appear in the results, neither of these runs produced a significant systematic effect which could be attributed to recoil scattering. An additional check on the effect of recoil scattering is discussed in the next section.

7. *Deviations from the Linear Stopping Power Relation*

As can be seen in Fig. 3 the stopping power curves actually begin to turn over at higher velocities within the range of recoil velocities used in the measurements. In addition, it is known[13] that at low velocities the nuclear scattering, discussed above, produces a marked increase in the stopping power above the linear relation (as indicated schematically in Fig. 3). These effects have been treated by the Brookhaven group[11,14] by fitting the stopping-power curves with the expression

$$-dE/dx=K_n(v_0/v)+K_e(v/v_0)-K_3(v/v_0)^3, \quad (10)$$

where $v_0=c/137$ and K_n, K_e, and K_3 are constants to be determined from empirical data. With this form for the stopping-power function the measured shift ratio becomes

$$F_m=\frac{\alpha_e}{\alpha_e+\tau}\left[1+\delta_t+(\delta_3-\delta_n)\left(1-\frac{\alpha_e}{\tau}\delta_t\right)\right], \quad (11)$$

where, as before, δ_t is the target correction. The characteristic slowing down time α_e is now derived from the linear coefficient K_e. The term δ_n which corrects for nuclear scattering is the same factor given by Warburton *et al.*[11] and can be obtained from their curves. The term δ_3, assumed small in Eq. (11), corrects for the turning over of the stopping-power curves and is given by

$$\delta_3=(K_3/K_e)(v/v_0)^2(\tau/(\alpha_e+3\tau)), \quad (K_3/K_e)\ll 1. \quad (12)$$

In applying Eq. (11) to the present measurements it is again necessary to average the correction factor over the initial velocity distribution and the target thickness. The measurements were all analyzed with the aid of Eq. (11). As it turned out, however, these refinements produced small modifications in the final results. As can be seen in Eq. (11) the δ_3 and δ_n corrections tend to cancel each other when they are approximately equal. Moreover, even when the nuclear correction δ_n is more important, its neglect in the linear analysis is compensated to a considerable extent by the use of α instead of α_e. As pointed out by Warburton,[15] the inclusion of the δ_n correction also takes into account the effects of recoil scattering if the coefficient K_n is selected so as to fit the measured range-energy curve (where range is defined as the projected distance at which the ion comes to rest).

8. *Contaminants*

The production of Be^7 and its subsequent decay to Li^{7*} is a possible source of error in the measurement of the Li^{7*} lifetime. This error was assessed in three ways. (1) From a knowledge of the pertinent cross sections, decay rates, and branching ratios it was estimated that the buildup of Be^7 during the runs (10–20 h) would produce less than a 1% error in the Li^{7*} lifetime. (2) After some of the runs this calculation was confirmed by counting the residual activity. (3) After one of the longest runs, the first observation made was repeated to see if any shift in the centroid of the Li^{7*} line could be detected. No shift was detected, the maximum uncertainty corresponding to less than 1% in the lifetime.

Based on the above considerations, the experimental procedure was as follows. A thin target of lithium metal (enriched to 99.7% in Li^7) was evaporated onto a nickel backing in the vacuum of the target chamber. The nickel backing was 140 keV thick to protons of 3.0 MeV. The thickness of each lithium target was determined by measuring a threshold curve for the reaction $Li^7(p,n)Be^7$. The shape of this curve could be used to obtain average values of the thickness for the thicker targets but not for the thinner ones.[16] Therefore, the thickness of a thin target was determined by comparing the yield in the resonance above threshold with that for a thick target. Figure 5 shows the threshold curves for a target taken before and after a run. All target thicknesses are expressed in terms of the threshold values.

The proton beams of energy 3.0 MeV were obtained from the Stanford 3-MeV Van de Graaff accelerator. The 478-keV gamma rays from Li^{7*} and the 432-keV gamma rays from Be^{7*} were observed with a Ge(Li) detector, 1 cm^2 in area and 0.3 cm deep. A Na^{22} source was used to obtain a reference line at 511 keV. Spectra were obtained for four arrangements: (1) with the detector at 0°, the target was oriented so that the beam passed through the nickel backing onto the target to

[14] E. K. Warburton, J. W. Olness, K. W. Jones, C. Chasman, R. A. Ristinen, and D. H. Wilkinson, Phys. Rev. (to be published).

[15] E. K. Warburton (private communication).

[16] J. E. Monahan and F. P. Mooring, Nucl. Instr. Methods 6, 343 (1960).

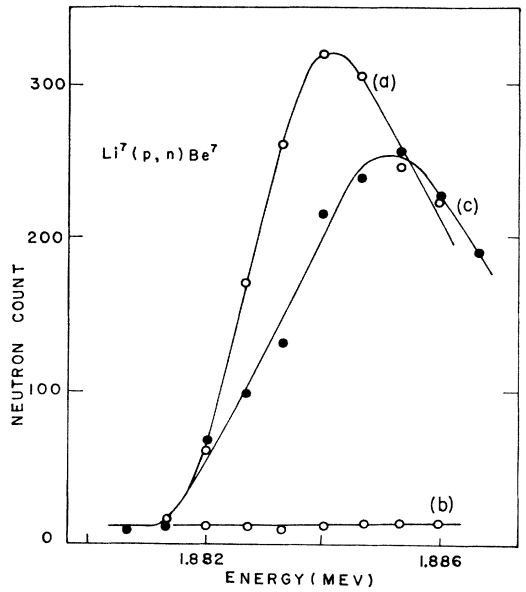

FIG. 5. Threshold curves for a target used in the determination of the Doppler shifts: (a) threshold curve obtained before the run; (b) curve obtained with the target reversed to test for the presence of lithium on the reverse side of the target; (c) threshold curve measured after the run. A thickness of 0.7±0.3 keV was found for this target from the strength of the resonance (not shown) above threshold.

allow the ions to recoil into vacuum; (2) the target was reversed so that the ions recoiled into the nickel; (3) the detector was shifted to 155° and the target reversed to obtain recoil into vacuum; (4) the target was then reversed once more to obtain recoil into nickel. At the end of some of the runs the $Li^7(p,n)Be^7$ threshold curve was rerun in order to determine the amount of deterioration of the target. A typical sequence of spectra is shown in Fig. 6. Five such runs were made for various target thicknesses. A sixth run was obtained with carbon, instead of nickel, as the stopping medium. Two more runs were obtained with a larger Ge(Li) detector, 6 cm^2 in area and 1 cm deep. In these runs a second reference line at 355 keV (from a Ba^{133} source) was employed. The proton beam in these observations was obtained from a newly installed 15-MeV FN-tandem Van de Graaff accelerator. One of these runs was made at a bombarding energy of 3.0 MeV; the other at a bombarding energy of 4.4 MeV.

TABLE I. Values of the shift ratio as measured, F_m, and corrected, F_c, for target thickness. The first seven measurements were made with nickel as the stopping medium, the last measurement with carbon. The bombarding energy was 3.0 MeV for all measurements except the fourth for which it was 4.4 MeV. The third and fourth runs were made with the larger Ge(Li) detector.

Target thickness (keV)	Li^{7*} F_m	$(1+\delta_l)^{-1}$	F_c	Be^{7*} F_m	$(1+\delta_l)^{-1}$	F_c
0.7±0.3	0.792	0.961	0.761±0.050	0.562	0.941	0.529±0.054
1.5±0.5	0.800	0.930	0.744±0.030	0.582	0.889	0.518±0.037
1.5±0.5	0.801	0.930	0.745±0.020	0.589	0.889	0.524±0.027
2.6±0.8	0.821	0.915	0.751±0.020	0.572	0.859	0.492±0.027
2.7±0.8	0.852	0.897	0.764±0.025	0.667	0.829	0.553±0.040
3.0±1.5	0.840	0.890	0.748±0.040	0.635	0.817	0.519±0.057
5.6±1.7	0.922	0.849	0.783±0.030	0.813	0.735	0.597±0.040
1.8±0.9	0.922	0.950	0.876±0.022	0.785	0.930	0.729±0.030

III. RESULTS

The spectra were analyzed with the aid of an electronic computer. A linear background, fitted to the data above and below a peak, was subtracted, and then the centroid of the peak was computed. The centroid was corrected for any shifts observed in the reference lines. The shift ΔE_c of Eq. (5) was calculated for vacuum and for stopping in a medium. Since the detection system was linear in energy to better than 1%, the ratio of the shifts F_m can be computed directly without conversion to energy. The results of the various measurements are given in Table I. The first column gives the target thickness determined from measurements on the $Li^7(p,n)Be^7$ threshold, as discussed above. The stated errors are believed to cover the uncertainties in the thickness determinations, as well as possible nonuniformities in the targets. The errors in the results include these uncertainties in the target thicknesses. The corrections for target thickness were obtained from Fig. 4, and applied to the measured values F_m to obtain the corrected values F_c given in Table I.

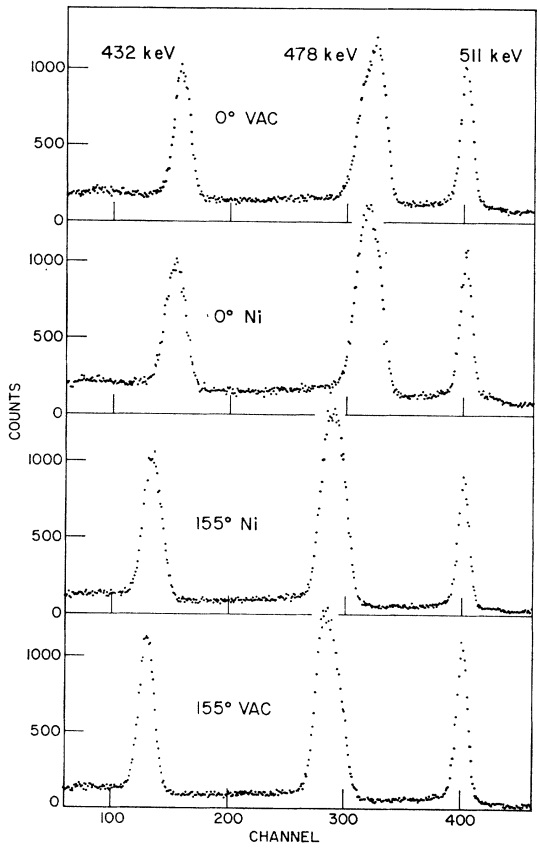

FIG. 6. Sequence of spectra obtained for the 2.7-keV thick target.

TABLE II. Stopping power data. The value for Li^7 in Ni from Teplova *et al.*[a] is based on a measurement at $v=3.7\times10^8$ cm/sec. All other values are obtained by interpolation.[b]

	$-(dE/dx)_{v=v_0}$ (keV/(μg/cm²)) Teplova *et al.*[a]	Porat *et al.*[c]	Mean α (10^{-13} sec)
Li^7 in Ni	0.55	0.58	3.16
Be^7 in Ni	0.82	0.78	2.23
Li^7 in C	1.09	1.55	6.51
Be^7 in C	1.37	2.11	4.94

[a] See Ref. 7.
[b] See Ref. 11.
[c] See Ref. 12.

The stopping power data used to obtain α are given in Table II. For stopping in nickel the agreement between the results of Tepolva *et al.*[7] and Porat and Ramavataram[12] is good, but for carbon there is substantial disagreement. Hence, the lifetimes derived from the measurements with carbon were not used in obtaining the final average values of the lifetimes. Nevertheless, it is believed that the *ratio* of the stopping powers for lithium and beryllium ions in carbon is probably not seriously in error, so that the good agreement of the lifetime ratios obtained with carbon and with nickel is significant. The values of F_c in Table I can be averaged and used with the values of α from Table II in the relation

$$\tau=\alpha(1-F_c)/F_c,$$

to obtain the following results based on a linear stopping power curve:

$$\tau_{Li^{7*}}=(1.03\pm0.14)\times10^{-13}\text{ sec},$$
$$\tau_{Be^{7*}}=(2.00\pm0.25)\times10^{-13}\text{ sec}.$$

Table III gives the coefficients used in the more refined description of the stopping power curve in Eq. (10). The coefficients K_n were obtained from the work of Warburton *et al.*[11] whenever possible and by plausible interpolation otherwise. The values of K_e and K_3 were next obtained by fitting measured or interpolated stopping power curves. The values of α_e are derived from K_e. The values of δ_n were obtained from the curves given by Warburton *et al.*[11] and the values of δ_3 from Eq. (12). Whenever appropriate these values were averaged over the velocity distribution in an approximate

TABLE III. Empirical values for the coefficients in the stopping power function, Eq. (10), and values of α_e and the correction factors derived from them.

	K_e (keV/(μg/cm²))	K_n	K_3	α_e (10^{-13} sec)	$\langle\delta_n\rangle$	$\langle\delta_3\rangle$
Li^7 in Ni	0.55	0.027	0.012	3.25	0.012	0.012
Be^7 in Ni	0.77	0.04	0.013	2.32	0.060	0.009
Li^7 in C	1.29	0.07	0.04	6.7	0.003	0.012
Be^7 in C	1.69	0.09	0.04	5.1	0.020	0.010

TABLE IV. Mean lifetimes of Li^{7*} and Be^{7*} measured with nickel and carbon backings. The values of F_c from Table I have been corrected for nonlinearity of the stopping power function and averaged to obtain the listed value of F_c.

	Backing	F_c	α_e (10^{-13} sec)	τ (10^{-13} sec)
Li^{7*}	Ni	0.754±0.016	3.25±0.33	1.06±0.14
	C	0.870±0.022	6.7 ±1.4	1.00±0.28
Be^{7*}	Ni	0.547±0.020	2.32±0.23	1.92±0.25
	C	0.733±0.030	5.1 ±1.1	1.85±0.48

manner. Equation (11) was then used to obtain the corrected values F_c listed in Table IV. The lifetimes obtained by use of the more refined stopping power function are:

$$\tau_{Li^{7*}}=(1.06\pm0.14)\times10^{-13}\text{ sec},$$
$$\tau_{Be^{7*}}=(1.92\pm0.25)\times10^{-13}\text{ sec}.$$

It is apparent that for lifetimes in this range and for the method and conditions selected for this investigation the analysis based on a linear stopping power function is quite accurate.

As discussed earlier, the data can also be treated by fitting calculated lines to the peaks observed for stopping in a medium. One example of this procedure is illustrated in Fig. 7. The 511-keV reference line indicates the resolution of the detector. The 432-keV line

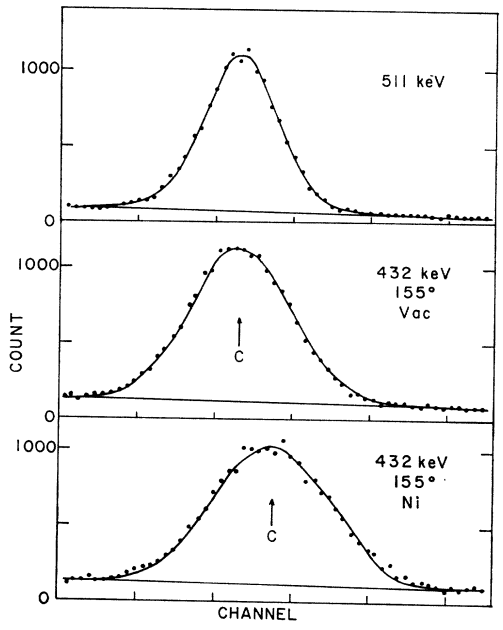

FIG. 7. Illustration of the observed line shapes. At the top the 511-keV line shows the detector resolution. In the middle the 432-keV line shows the Doppler broadening due to the velocity spread for recoils traveling in vacuum. At the bottom the line observed for recoils stopping in nickel has been fitted by a curve generated by folding the "vacuum" curve into the function of Eq. (8). Values of $\tau=1.95\times10^{-13}$ sec and $\alpha_e=2.30\times10^{-13}$ sec were used to obtain the fit. The fitted curve is also modified for computed values of the target correction δ_t and the nuclear correction δ_n.

observed at 155° for free recoil is used as the "prompt" resolution function which is folded into Eq. (8) to generate the shifted line corresponding to recoil into nickel. To obtain the fit shown it was necessary to include both the target correction δ_t and the nuclear correction δ_n. In fact, it was found that the fit depends rather sensitively and independently on τ, δ_t, and δ_n. Decay in the target contributes an unshifted component to the peak and produces much of the yield on the low-energy side (for $\theta=155°$) and hence broadens the peak. Decay in the nickel provides the shifted, but essentially unbroadened component which predominates throughout the remainder of the peak. Thus the fit in this region is sensitive to the lifetime. However, the actual slope on the high-energy side is altered by the nuclear stopping term which has the effect of shifting yield from the high to the low part of the slope. The satisfactory agreement obtained in fitting the shifted peak in Fig. 7 supports the result of the centroid analysis and the essential validity of the corrections used.

Finally, the experimental values of $\langle v_z \rangle$, obtained from Eq. (5) for free recoil, agree well with values computed from the kinematics and the measured angular distributions[17,18] of the reaction products, as shown in Table V.

TABLE V. Comparison of experimentally measured and computed values of $\langle v_z \rangle$.

	$\langle v_z \rangle$ (10^8 cm/sec) Experimental	Computed	Angular distribution
Li^{7*}	3.35±0.10	3.24±0.12	[a]
Be^{7*}	2.86±0.09	2.91±0.06	[b]

[a] Reference 18.
[b] Reference 17.

IV. DISCUSSION

The measured lifetimes are compared with earlier results in Table VI. The value obtained for Li^{7*} is in better agreement with the measurements obtained by resonance fluorescence than with the values obtained in previous Doppler-shift measurements. The value found for Be^{7*} is within the limits of error of the earlier Doppler-shift measurement, but it is considerably lower and more precise than the latter measurement. For Li^{7*} we adopt an average of the present measurement and the results from resonance fluorescence:

$$\tau_{Li^{7*}}=(1.10\pm0.10)\times10^{-13}\text{ sec}.$$

Since the present experiment determines the ratio of the lifetimes with more precision than it does their absolute values, we adopt for Be^{7*} a value based on the measured ratio and the adopted value for Li^{7}:

$$\tau_{Be^{7*}}=(2.00\pm0.26)\times10^{-13}\text{ sec}.$$

TABLE VI. Comparison of mean lifetimes of Li^{7*} and Be^{7*} with previous measurements and with theoretical calculations.

Li^{7*} (10^{-13} sec)	Be^{7*} (10^{-13} sec)	Ratio	Method[a]	Reference
0.75±0.25			DS	Elliott and Bell[b]
0.77±0.08	2.7 ±1	3.50±1.4	DS	Bunbury *et al.*[c]
1.1 ±0.3			RF	Beckman and Sandstrom[d]
1.15±0.14			RF	Swann *et al.*[e]
1.25±0.06			RF	Mouton *et al.*[f]
0.93±0.12			RF	Booth *et al.*[g]
1.06±0.14	1.92±0.25	1.82±0.20	DS	This work
1.10±0.10	2.00±0.26	1.82±0.20	DS, RF	Adopted
1.15	2.13	1.85	Theor	Barker[h]
1.18			Theor	Cohen and Kurath[i]

[a] DS = Doppler shift; RF = resonance fluorescence.
[b] Reference 1.
[c] Reference 2.
[d] Reference 3.
[e] Reference 4.
[f] Reference 5.
[g] Reference 6.
[h] Reference 9.
[i] Reference 8.

Theoretical values for the lifetimes and their ratio have been computed by Lane,[19] as a function of the degree of intermediate coupling in the mass-7 nuclei. His results are shown graphically in Fig. 8 along with the adopted experimental values. It is seen that the experimental values indicate that L-S coupling is favored in these nuclei, in agreement with other evidence.[19,20] The experimental values are also in excellent agreement with those predicted by Cohen and

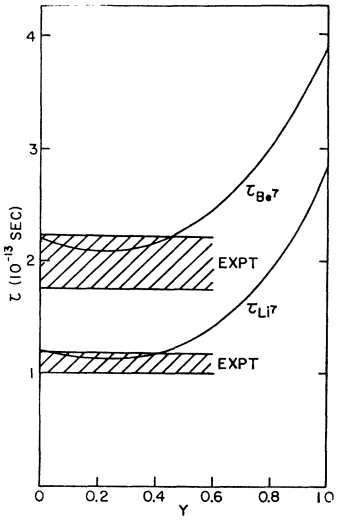

FIG. 8. Comparison of the adopted values of the lifetimes of Li^{7*} and Be^{7*} with the calculations of Lane (Ref. 14). The parameter γ, equal to $(a/K)/[(a/K)+5]$, expresses the relative strengths of central and spin-orbit forces in intermediate coupling.

[17] R. Gleyvod, N. P. Heydenburg, and I. M. Naqib, Nucl. Phys. 63, 650 (1965).
[18] P. R. Bevington, W. W. Rolland, and H. W. Lewis, Phys. Rev. 121, 871 (1961).
[19] A. M. Lane, Proc. Phys. Soc. (London) A68, 189 (1955); Rev. Mod. Phys. 32, 519 (1960).
[20] D. Kurath, Phys. Rev. 101, 216 (1956).

Kurath[8] in their study of the complete p-shell and by Barker[9] in his study of the lithium and beryllium nuclei, as shown in Table VI. The excellent agreement between the measured value of the lifetime ratio and that predicted for strong L-S coupling is especially satisfying. The earlier and much larger experimental value of the ratio had raised doubts[2,19] as to the validity of calculations which neglect the motion of the core in these nuclei.

ACKNOWLEDGMENTS

We would like to thank G. D. Sprouse for his generous assistance and interest in this work. We are grateful to L. G. Mann, D. C. Camp, and G. A. Armantrout of the Lawrence Radiation Laboratory, Livermore, for making available to us the large Ge(Li) detector used in part of the work. We would also like to thank P. R. Bevington for his advice in the use of the PDP-7 computer.

PHYSICAL REVIEW VOLUME 147, NUMBER 3 22 JULY 1966

Beta-Delayed Protons from Si^{25}†

P. L. REEDER,* A. M. POSKANZER,‡ R. A. ESTERLUND, AND R. MCPHERSON
Chemistry Department, Brookhaven National Laboratory, Upton, New York
(Received 3 March 1966)

Silicon-25 was produced by the $Mg^{24}(He^3,2n)Si^{25}$ reaction with a 32-MeV He^3 beam. The beta-delayed proton spectrum was measured from 0.7 to 6.0 MeV, with a resolution of 85 keV full width at half-maximum above 1.7 MeV. Eighteen proton peaks are identified and assigned to transitions from virtual levels of Al^{25}. Three new levels of Al^{25} at 6.92±0.04, 7.25±0.03, and 8.20±0.03-MeV excitation energy are proposed in addition to the $T=\frac{3}{2}$ analog state at 7.90±0.02 MeV and a state at 8.97±0.04 MeV which had been seen in previous delayed-proton work. The Si^{25} half-life was determined to be 218±4 msec.

INTRODUCTION

SILICON-25 was one of the first isotopes reported to decay by beta-delayed proton emission.[1] Among the light elements a series of nuclides ranging from C^9 to Ti^{41} have also been shown to exhibit this mode of decay.[2] These nuclides have beta-decay half-lives less than 0.3 sec. They are produced by nuclear reactions using pulsed beams and the proton spectra are observed between beam pulses with solid-state detectors. In the case of Si^{25}, allowed beta transitions populate states of Al^{25} which then emit protons if the excitation energy of the state is greater than the proton separation energy of Al^{25} which is 2.29 MeV. Because the first excited state in the final nuclide Mg^{24} is only 1.37 MeV above the ground state, proton emission from higher excited states of Al^{25} may go to either the ground or first-excited state. Thus the proton spectrum may be doubled relative to the number of states populated by beta decay. McPherson and Hardy[3] measured the half-life of Si^{25} to be 225±6 msec and reported at least four and possibly six groups in the proton spectrum. They assigned two of their proton peaks to a known level in Al^{25} at 7.14 MeV and two other proton peaks to a new level at 7.93 MeV. The new level was assumed to be the analog state of the ground state of Si^{25} since the logft for the beta transition was significantly less than the logft for the 7.14-MeV level. Similar analog-state peaks have now been seen in most of the other beta-delayed proton spectra.[4] Later results of Hardy and Bell for Si^{25} put the new level at 7.91 MeV and suggested that two more peaks were present arising from transitions from a proposed level at 9.03 MeV.[5] Delayed protons from Si^{25} have also been observed by Bender, Williams, and Toth.[6]

The level structure of Al^{25} has been studied by proton elastic and inelastic scattering on Mg^{24}, and many levels have been found above the proton separation energy.[7] In the more extensively studied mirror nucleus, Mg^{25}, sixty levels have been seen in this region.[8] If some of these levels are populated by allowed beta decay, the delayed-proton spectrum should be far more complex than has been previously reported. We have measured the delayed-proton spectrum of Si^{25} with a resolution

† Research performed under the auspices of the U. S. Atomic Energy Commission.
* Present address: Chemistry Department, Washington University, St. Louis, Missouri.
‡ Present address: Lawrence Radiation Laboratory, Berkeley, California.
[1] R. Barton, R. McPherson, R. E. Bell, W. R. Frisken, W. T. Link, and R. B. Moore, Can. J. Phys. **41**, 2007 (1963).
[2] R. McPherson, R. A. Esterlund, A. M. Poskanzer, and P. L. Reeder, Phys. Rev. **140**, B1513 (1965), and references therein.
[3] R. McPherson and J. C. Hardy, Can. J. Phys. **43**, 1 (1965).
[4] J. C. Hardy and B. Margolis, Phys. Letters **15**, 276 (1965).
[5] J. C. Hardy and R. E. Bell, Can. J. Phys. **43**, 1671 (1965).
[6] R. S. Bender, I. R. Williams, and K. S. Toth, Nucl. Instr. Methods **40**, 241 (1966).
[7] Data for Al^{25} have been taken primarily from P. M. Endt and C. Van der Leun, Nucl. Phys. **34**, 1 (1962) with additions from T. Lauritsen and F. Ajzenberg-Selove, *Energy Levels of Light Nuclei* (National Academy of Science–National Research Council, Washington, D. C., 1962), and corrections from W. T. Joyner, Phys. Rev. **128**, 2261 (1962).
[8] R. K. Sheline and R. A. Harlan, Nucl. Phys. **29**, 177 (1962).